ELSEVIER

Chemical Engineering Journal 109 (2005) 57–66

Chemical Engineering Journal
www.elsevier.com/locate/cej

The behaviour of a low-productive non-pretreated V_2O_5–TiO_2 (anatase) catalyst for oxidation of *o*-xylene to phthalic anhydride

Asen I. Anastasov*

Institute of Chemical Engineering, Bulgarian Academy of Sciences, Acad. G. Bontchev Street, Bl. 103, 1113 Sofia, Bulgaria

Received 4 May 2004; received in revised form 8 March 2005; accepted 15 March 2005

Abstract

The behaviour of a low-productive V_2O_5–TiO_2 (anatase) supported catalyst for oxidation of *o*-xylene to phthalic anhydride is investigated. The catalyst operates by inlet reagent concentration $40\,g\,m^{-3}$(STP) (usual concentration in the industry) and is calcined under conditions, which differ in comparison with those applied in the industry. It is experimentally specified that the amount of the vanadium chemically bonded with the TiO_2 support depends considerably on the conditions of calcination. Experiments are carried out in a pilot installation with a fixed catalyst bed composed by a catalyst, which is calcined, but has not undergone other preliminary operations. The dependence of the hot spot temperature on the variation of the process parameters is studied. By means of a heterogeneous two-dimensional model an identification problem is solved. As a result the energies of activation valid for the calcined catalyst are determined. It is found that a calcined but not pretreated sample is considerably more active than the pretreated form. A brief statistic analysis of the experimental and predicted results is performed.

Keywords: Identification problem; Kinetic parameters; Fixed bed; Simulation; *o*-Xylene

1. Introduction

The oxidation of *o*-xylene to phthalic anhydride is one of the most important industrial processes and therefore the leading researchers go on with it [1–3]. Lately, the engineers carry out the process by using modern, high-productive catalysts [4,5]. But several years ago, the catalyst O 4-25 operated at *o*-xylene concentration $40\,g\,m^{-3}$ (STP) was intensively used. Up to now it has not lost significance and is used in many chemical plants all over the world [4]. This is due to its low price, high thermal stability and good qualities tested many times in the industry. Moreover, the inlet reagent concentration for this catalyst does not exceed the lower explosion limit of the reaction mixture (about 1 mol% *o*-xylene in air) [4].

We have devoted many papers to the realisation of the oxidation process, as well as to its equipment [6–8]. Our last studies concern the high-productive catalysts O 4-26 and O 4-28 [5,9], especially their kinetics and deactivation under industrial conditions. Nevertheless, our interest to the conventional catalyst does not wane, which is due to its specific nature. In a recent paper [10] we made an attempt to compare together two forms of the catalyst O 4-25 (pretreated and non-pretreated) with respect to the parametric sensitivity (PS) of the process. In contrast to the highly productive catalysts (inlet *o*-xylene concentration 60 and $80\,g\,m^{-3}$ (STP)), which are not subjected to any preliminary treatments, the O 4-25 catalyst undergoes a two months treatment before being introduced in a regular exploitation. On the other hand, it is well known that the PS problems are especially important with respect to the realisation of an exothermic catalytic process in a fixed catalyst bed. Situations exist, when small variations of the process parameters cause significant changes of the temperature regime accompanied by a sharp increase of the hot spot temperature [11–13]. The last one is especially unfavourable for the characteristics of both the process and the catalyst.

In the paper mentioned [10] it was established that the operation with a catalyst, which is calcined, but not com-

---

* Tel.: +359 2 979 34 80; fax: +359 2 870 75 23.
E-mail addresses: aia@ice.bas.bg, chimreac@bas.bg (A.I. Anastasov).

1385-8947/$ – see front matter © 2005 Elsevier B.V. All rights reserved.
doi:10.1016/j.cej.2005.03.010

Nomenclature

a	specific external surface area of pellets ($m^2\,m^{-3}$)
C	concentration of component in gas phase ($kmol\,m^{-3}$)
C_g	heat capacity of gas ($J\,m^{-3}\,K^{-1}$)
C_p	concentration of component on the surface of pellets ($kmol\,m^{-3}$)
C_0	inlet concentration of component in gas phase ($kmol\,m^{-3}$) ($g\,m^{-3}$(STP)) (m^3(STP) defined as m^3 at 0 °C and 101.325 kPa)
D_r	coefficient of effective mass diffusivity in radial direction for gas ($m^2\,s^{-1}$)
E	energy of activation ($kJ\,kmol^{-1}$)
F	dimensionless Fiescher number
F_A	dimensionless factor accounting for in a formal way the catalyst activity along the bed
F_t	dimensionless tabulated Fiescher number
h_{gc}	heat transfer coefficient between fixed bed and coolant ($W\,m^{-2}\,K^{-1}$)
h_{gp}	heat transfer coefficient between gas and catalyst pellets ($W\,m^{-2}\,K^{-1}$)
ΔH	heat effect of corresponding reaction ($J\,kmol^{-1}$)
k_{gp}	mass transfer coefficient between gas and catalyst pellets ($m\,s^{-1}$)
K	reaction rate constant ($kmol\,kg^{-1}\,s^{-1}\,Pa^{-1}$)
K_C	rate constant of catalyst reoxidation ($kmol\,kg^{-1}\,s^{-1}\,Pa^{-1}$)
K_0	pre-exponential factor ($kmol\,kg^{-1}\,s^{-1}\,Pa^{-1}$)
l	axial coordinate (m)
L	length of bed (cm)
P	partial pressure of component (Pa)
P_{ox}	partial pressure of oxygen (Pa)
r	radial coordinate (m)
r_p	reaction rate by steps on catalyst pellets ($kmol\,kg^{-1}\,s^{-1}$)
R	tube radius (m)
S_r	variance of experimental and predicted results (°)
T	temperature of gas (K)
T_c	temperature of coolant (accepted to be equal to the temperature of the tube wall) (K) (°C)
T_{fb}	temperature in bed (measured experimentally) (°C), as well as mean temperature (obtained from arithmetic means of temperatures of gas and solid phases) for model prediction (°C)
T_{hs}	temperature of hot spot (measured experimentally) (°C), as well as mean temperature of hot spot (obtained from arithmetic means of hot spot temperatures of gas and solid phases) for model prediction (°C)
T_p	temperature of pellets (K)
T_0	inlet temperature of gas (K) (°C)
V	flow rate of reaction mixture per single tube (m^3(STP) h^{-1})
V_b	gas velocity with respect to full cross section of tube ($m\,s^{-1}$)
W_p	reaction rate by component on catalyst pellets ($kmol\,kg^{-1}\,s^{-1}$)

Greek letters

α	defined in Eq. (13) (dimensionless)
ε	void fraction of fixed bed (dimensionless)
λ_r	coefficient of effective conductivity in radial direction for gas ($W\,m^{-1}\,K^{-1}$)
$\nu_1,\ \nu_2$	ranges of discretion (dimensionless)
ρ_p	density of pellets ($kg\,m^{-3}$)
σ_{n-1}	variance of reproducibility of hot spot experimental temperatures (°C)

Subscripts

A	*o*-xylene
B	*o*-tolualdehyde
C	phthalide
D	phthalic anhydride
i	component (1 = A; 2 = B; 3 = C; 4 = D)
m	reaction step

pletely pretreated, leads to very high hot spot temperatures exceeding or being quite near to the maximum admissible temperature for the V_2O_5–TiO_2 (anatase) system (500 °C). But a quantitative analysis of the high catalyst activity was not given, nor yet an attempt to work out its kinetics was done. This is important with a view to evaluate the opportunities for the process realisation by using the calcined form under industrial regime, which is different in comparison with the pretreated sample [14]. Moreover, if kinetics for such a catalyst form is available, the precise determination of the parametric sensitivity at various industrial situations will be solved.

Thus, the aim of this paper is to determine the kinetic parameters valid for a calcined catalyst by using the kinetic model for oxidation of *o*-xylene suggested by Calderbank et al. [15]. In order to achieve it, we solved an identification problem by means of a proper mathematical model and using experimental data obtained in a pilot set-up. The experiments concern the hot spot temperatures in a fixed bed constituted by a non-pretreated (only calcined) sample. They are obtained as a function of various process parameters, namely cooling temperature T_c, inlet temperature of the reaction mixture T_0, initial *o*-xylene concentration $C_{A,0}$ and gas flow rate through a single contact tube V.

Regardless of the fact that kinetic problems are studied here, they are solved by using typical methods of the reaction engineering. Therefore, the reaction engineering aspects of this study should be especially important for the reader.

2. Experimental

2.1. Industrial reactor

The experiments related to the behaviour of the catalyst in the beginning (third day) and at the end (50th day) of the real pretreatment (taking place after the stage of calcination) was carried out in an industrial reactor, whose scheme was shown in our paper [16]. The apparatus has 8920 contact tubes of 3250 mm length and 26 mm inner diameter, as well as a built-in steam generator. The reactions' heat is removed by a coolant, an eutectic mixture of KNO_3 and $NaNO_2$ (ratio 57:43) circulating in the shell-side. More details about the conventional reactor are given in [7,17].

2.2. Pilot experimental installation

The first stage of the pretreatment of a fresh catalyst O 4-25 or of its calcination, as well as the experiments using the calcined form were performed in a pilot installation depicted Fig. 1. Its most important element, the integral non-isothermal, non-adiabatic reactor (2) is identical with a single tube of the industrial unit. The maintenance of a proper tube wall temperature is achieved through electric heaters (3) located around the tube and grouped in eight sections. Each section is connected to a positional thermoregulator and an iron–constantan thermocouple. They both control the wall temperature. A mobile NiCr–Ni thermocouple (supplied with a data logger) installed coaxially in the centre of the tube measures the temperature in the bed. Temperature measurements in the catalyst bed are performed several hours after reaching a stationary regime. The installation contains also a preheater of the air and an evaporator of *o*-xylene assembled in the apparatus (1), a water-cooled condenser (4), and a scrubber (5). The raw phthalic anhydride is separated in (4), while the final cleaning of the air leaving the tube is realised in (5). A dosing pump (MMS-4, made in Czech Republic) with four pistons performs the dosage of *o*-xylene. All pipelines are heated to a temperature over 200 °C to prevent a condensation of the reaction products.

2.2.1. Catalyst

The physicochemical characteristics of the conventional V_2O_5–TiO_2 (anatase) supported catalyst operated at inlet *o*-xylene concentration $40\,g\,m^{-3}$(STP), as well as the indices of the bed in both the industrial and pilot reactors are [16]:

- specific catalyst surface: $10\,m^2\,g^{-1}$;
- specific volume of the pores (Hg): 269 $(m^3\,kg^{-1})\,10^6$;
- V/Ti ratio by weight: about 0.06;
- promoters: P_2O_5, Al_2O_3;
- bed density: $1500\,kg\,m^{-3}$;
- bed porosity: about 0.4;
- amount of the catalyst in a single tube: about 2100 g;
- bed height: 280 cm;
- thickness of catalyst layer: about 0.1 mm;
- support; porcelain spheres of diameter: 6 mm.

2.3. Analyses

The analyses of *o*-xylene, phthalic anhydride and side products *o*-tolualdehyde and phthalide are done by using gas chromatography (gas chromatograph Perkin-Elmer 8500). The maleic anhydride content is performed polarographi-

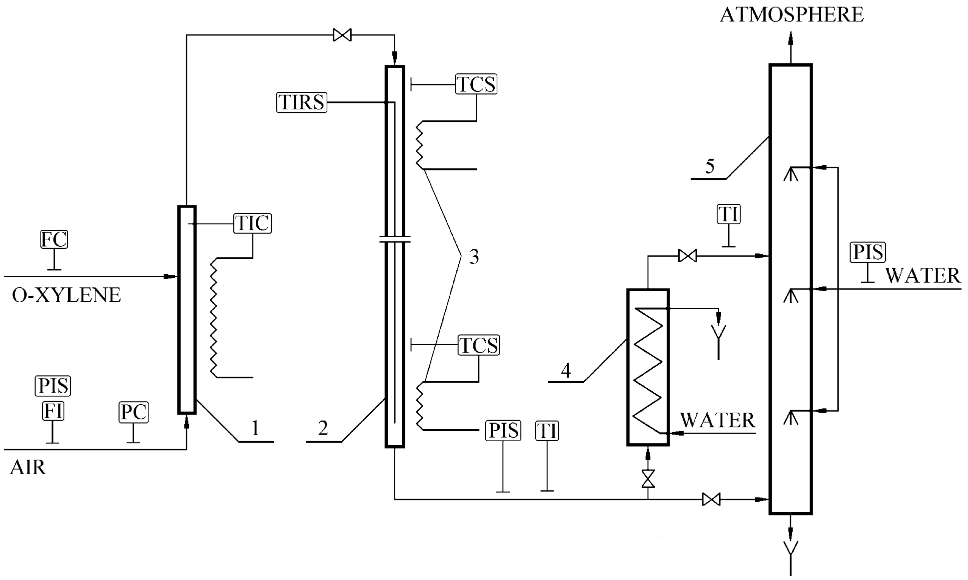

Fig. 1. Experimental set-up: C, control; F, fluid; I, information; P, pressure; R, registration; S, interlock; T, temperature; 1, preheater for air and evaporator for *o*-xylene; 2, pilot non-isothermal, non-adiabatic reactor; 3, electric heaters (eight pieces); 4, water-cooled condenser and 5, scrubber.

cally. The specific catalyst surface is determined through low-temperature adsorption of N_2, while the elemental composition is specified by means of atomic adsorption spectrometry (AAS). A DRON-3 diffractometer (Cu Kα radiation) is used to specify the catalyst phase composition.

3. Mathematical model

As in our other communications [9,10,17] a two-dimensional heterogeneous model describing the behaviour of the gas and solid phases is used in this study. It was suggested by Froment [18] and is recognised as most suitable to study highly exothermic catalytic processes with chemical reactions running on the catalyst surface [19–21]. For a single contact tube of cylindrical form under stationary conditions the model is presented by the following equations:

Gas phase

$$D_{r,i}\left(\frac{\partial^2 C_i}{\partial r^2}+\frac{1}{r}\frac{\partial C_i}{\partial r}\right)-V_\mathrm{b}\frac{\partial C_i}{\partial l}+k_{\mathrm{gp},i}a(C_{\mathrm{p},i}-C_i)=0 \tag{1}$$

$$\lambda_r\left(\frac{\partial^2 T}{\partial r^2}+\frac{1}{r}\frac{\partial T}{\partial r}\right)-V_\mathrm{b}C_\mathrm{g}\frac{\partial T}{\partial l}+h_\mathrm{gp}a(T_\mathrm{p}-T)=0 \tag{2}$$

with boundary conditions:

$$l=0; \qquad C=C_{0,i}; \qquad T=T_0 \tag{3}$$

$$r=0; \qquad \frac{\partial C_i}{\partial r}=0; \qquad \frac{\partial T}{\partial r}=0 \tag{4}$$

$$r=R; \qquad \frac{\partial C_i}{\partial r}=0; \qquad -\lambda_r\frac{\partial T}{\partial r}=h_\mathrm{gc}(T-T_\mathrm{c}) \tag{5}$$

Catalyst pellets:

$$k_\mathrm{gp}a(C_i-C_{\mathrm{p},i})+W_{\mathrm{p},i}(C_{\mathrm{p},i},T_\mathrm{p},F_\mathrm{A}(l))\rho_\mathrm{p}(1-\varepsilon)=0 \tag{6}$$

$$h_\mathrm{gp}a(T-T_\mathrm{p})+\sum_{m=1}^{s}r_{\mathrm{p},m}(C_{\mathrm{p},i},T_\mathrm{p},F_\mathrm{A}(l))\rho_\mathrm{p}(1-\varepsilon)(-\Delta H_m)=0 \tag{7}$$

The system (1)–(7) is approximated by an implicit finite-difference scheme and solved by using the false-transient method. More details about the solution are presented in our communication [22]. The model coefficients D_r, λ_r, k_gp, h_gp and h_gc are determined with the help of the relationships given in [23], while some concrete values are shown in [9].

4. Kinetics

In this study, as well as in the case of determining the kinetics of the catalysts O 4-26 and O 4-28 [5], we used the kinetic scheme and equations suggested by Calderbank et al. [15]. There is an unanimous opinion that they are among the best ones for the oxidation process [6,20,24] and give a good approximation to the real situation observed in the industrial reactor. According to its authors this kinetics is valid for various commercial V_2O_5–TiO_2 (anatase) supported catalysts, whatever the catalyst O 4-25 is. An undoubted advantage is the recognition of phthalide, which, as known, defines the quality of the raw phthalic anhydride. In our opinion, a considerable failing is the neglecting of maleic anhydride generation [25]. This substance is related to the products of combustion.

So, the network is [15]:

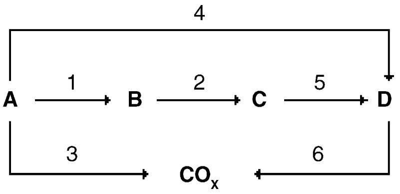

where A, B, C and D are *o*-xylene (*o*-XL), *o*-tolualdehyde (*o*-TA), phthalide (PH) and phthalic anhydride (PA). As it is suggested [15], the stage 6 is insignificant and can be neglected.

The kinetic equations by stages in partial pressures are:

$$r_{\mathrm{p},1}=K_1\alpha P_\mathrm{A} \tag{8}$$

$$r_{\mathrm{p},2}=K_2\alpha P_\mathrm{B} \tag{9}$$

$$r_{\mathrm{p},3}=K_3\alpha P_\mathrm{A} \tag{10}$$

$$r_{\mathrm{p},4}=K_4\alpha P_\mathrm{A} \tag{11}$$

$$r_{\mathrm{p},5}=K_5\alpha P_\mathrm{C} \tag{12}$$

Table 1
Original kinetic parameters and kinetic parameters defined for a catalyst O 4-25 calcined 72 h at 480 °C

Stage #	Original kinetic parameters according to Calderbank et al. [15]		Energies of activation for a catalyst calcined 72 h at 480 °C	Ratio of original to new energies of activation
	$K_{0,m}$ (kmol kg^{-1} s^{-1} Pa^{-1})	E_m (kJ kmol^{-1})	$E_{m,\mathrm{new}}$ (kJ kmol^{-1})	$E_{m,\mathrm{or.}}/E_{m,\mathrm{new}}$
1	3.7779×10^{-5}	61420	41282 ± 4463	1.488
2	5.4870×10^{-6}	46473	26335 ± 4463	1.765
3	3.5330×10^{-6}	51205	31066 ± 4463	1.648
4	1.2780×10^{-5}	54512	34374 ± 4463	1.586
5	3.1482×10^{-5}	57945	37807 ± 4463	1.533

where:

$$\alpha = \frac{K_C P_{ox}}{K_C P_{ox} + (K_1 + 6.5K_3 + 3K_4)P_A + K_2 P_B + K_5 P_C} \tag{13}$$

The value of $K_C P_{ox}$ by oxidation with air at near atmospheric pressure is 0.722×10^{-5} kmol kg^{-1} s^{-1}. The original values of the pre-exponential factors and energies of activation obtained by Calderbank et al. [15] are shown in Table 1, columns 2 and 3.

5. Results and discussion

5.1. Pretreatment procedure for the catalyst O 4-25

In order to account for the behaviour of the non-pretreated catalyst, it is worthwhile to remember here, what is the pretreatment procedure for a fresh sample. We used it in the industrial reactor [16].

As demonstrated theoretically and experimentally in [16], this operation is necessary to achieve a suitable activity of the fresh sample before its introduction into regular operation during 3–3.5 years. It is worth noting here that the form mentioned has initially a very low activity [16]. So, the complete cycle of the catalyst pretreatment under industrial conditions in the industrial reactor consists of two stages as follows.

- *First stage*: *Calcination*: As suggested, for the sake of convenience, this procedure is described below in the beginning of Section 5.3.
- *Second stage*: *Catalyst pretreatment*: After calcination, the air is mixed with *o*-xylene and the catalyst is treated during 50–60 days in the industrial reactor under strictly defined conditions. Using a fixed scheme [16] both the gas flow rate and the inlet reagent concentration increase gradually to the final industrial values 4.5 m^3(STP) h^{-1} and 40 g m^{-3}(STP) starting from 2.5 m^3(STP) h^{-1} and 27 g m^{-3}(STP), respectively. At the same time the cooling temperature decreases from 390 to 370–372 °C (industrial cooling temperature) at the end of the period. In fact, this operation is the real catalyst pretreatment.

It was established that a highly active monolayer of V_2O_5 chemically bonded with the TiO_2 support [26–28] was formed during the calcination of the sample (first stage). At present it is considered that just this layer is responsible for the activity and the selectivity of the catalyst in the process of *o*-xylene oxidation to phthalic anhydride [28–31]. Along with the formation of the monolayer small amount of free crystallites V_2O_5 having considerably lower activity are generated [32]. The creation of the monolayer is a very sensitive process with respect to its temperature and duration, which is also confirmed by del Arco et al. [33]. By varying the parameters mentioned these authors have established that the catalytic surface changes.

During the real catalyst pretreatment an artificial reduction of the activity is achieved in the first 60–80 cm of the bed. We specified [16] that at the end of the procedure it amounts to 0.7–0.8 of the activity in the remaining part of the bed. The deactivation discussed leads to a “quasi dilution” of the front portion of the bed, thus avoiding the real dilution in the hot spot area by inert materials as suggested in the literature [19,34]. A considerably softer temperature regime is realised in the reactor.

5.2. Behaviour of a catalyst O 4-25 pretreated under industrial conditions

The experimental temperature profiles obtained by the catalyst at the third day of the pretreatment (filled circles) and at the end of this procedure (50th day, blank circles) are shown in Fig. 2. In the same figure the temperature regimes predicted by the model with the original kinetic parameters [15] under conditions as for the experiments are also given. Curve 1 concerns the third day of the pretreatment, while curve 2 is related to the end of this period. Taking into consideration the good correspondence between predicted and experimental temperature regimes, it can be maintained that the kinetics of Calderbank et al. [15] interprets quite satisfactorily the catalyst behaviour. This concerns not only the temperature and the location of the hot spot, but also the calculated yield of PA and the contents of the side products. According

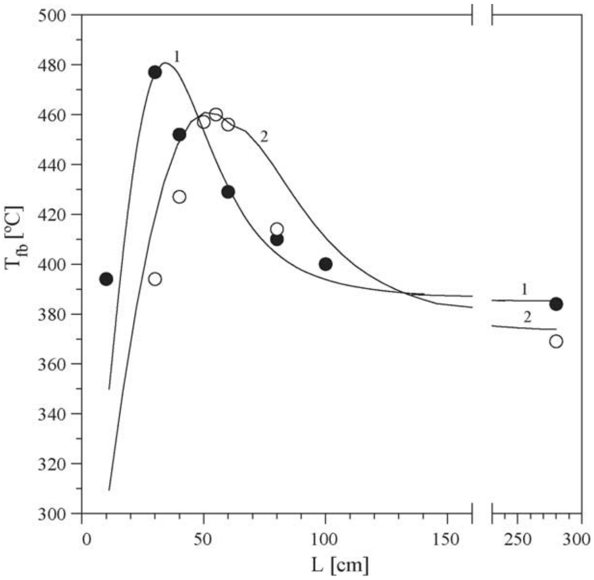

Fig. 2. Experimental and predicted temperature profiles in an industrial reactor of fixed bed (catalyst O 4-25). Filled circles: experimental temperatures ($r = 0$) at the third day of the real pretreatment; $V = 3.0$ m^3(STP) h^{-1}, $C_{A,0} = 31.5$ g m^{-3}(STP), $T_0 = 247$ °C, $T_c = 385$ °C. Blank circles: experimental temperatures ($r = 0$) at the end of the real pretreatment (50th day); $V = 4.5$ m^3(STP) h^{-1}, $C_{A,0} = 40$ g m^{-3}(STP), $T_0 = 230$ °C, $T_c = 372$ °C. Curve 1: model predictions under technological conditions as in the experiments marked by filled circles, $F_A = 1.08$ (0–60 cm), $F_A = 1$ (60–280 cm); curve 2: model predictions under technological conditions as in the experiments marked by blank circles, $F_A = 0.8$ (0–60 cm), $F_A = 1$ (60–280 cm).

to the simulation results (74 mol% for curve 2 and 79 mol% for curve 1), the PA yields correspond well with those determined experimentally (74–77 mol%). In regard to the side products, the calculations show a content of *o*-TA being about and a little more than 1 mol%, while the experimental yield is 0.6–0.8 mol%. The differences for phthalide are higher—the prediction shows about 4 mol%, but the experimental content is about four to five times lower (0.8–1 mol%). In fact, our industrial experience [17,22], confirms also the ability of the original kinetics to predict the behaviour of the pretreated catalyst.

5.3. Behaviour of a calcined catalyst O 4-25

In the stage of calcination (first stage of the pretreatment) the fresh catalyst is heated by hot air (without *o*-xylene) to 380–400 °C at a rate of 5–8 °C h^{-1}. The heating continues 4–6 h at this temperature at air flow rate 2.5 m^3(STP) h^{-1} per contact tube. This procedure is observed in the industrial reactor.

Bearing in mind the information about the high sensitivity of the calcination process towards its temperature and duration [33], we decided to carry out the calcination under conditions quite different than those typical of the industrial calcination. The aim was to see how the new conditions should affect the activity of the sample. As discussed above, the normal catalyst activity (assumed to be unity) is achieved just in the stage of calcinations [16].

The calcination was performed in the pilot set-up (Fig. 1) during 72 h at temperature 480 °C. These conditions differ significantly from the industrial calcination regime carried out at 380–400 °C during 4–6 h.

In the next four figures (Figs. 3–6) it can be seen the dependence of the hot spot temperatures on the variation of the parameters T_c, T_0, $C_{A,0}$ and V. The experimental results (circles) were obtained in a bed constituted by a catalyst, which was subjected only to a calcination procedure under the conditions specified above. The curves represent the simulation results in various situations discussed below.

Fig. 3 shows how the hot spot temperature changes when the cooling temperature increases. Curve 3 represents the model solution for a pretreated form calcined under industrial conditions. It makes an impression that the differences between the hot spot temperatures of the calcined catalyst and those of the pretreated sample are significant and range from 84 to 122 °C. Additional calculations (not given here) show that these differences are considerably higher than they should be if the activity of the calcined catalyst is two or three times higher than the activity of the pretreated form. As expected, if the activity of the calcined sample is two times higher ($F_A = 2$ along the whole bed height), the hot spot temperatures increase (Fig. 3, curve 4). Nevertheless, they remain considerably lower in comparison with those determined experimentally (differences between 72 and 93 °C). At the same time, in the first three days of the real pretreatment (72 h) the sample located in the hot spot zone (Fig. 2, filled circles) is under the influence of temperatures in the interval 450–480 °C. In other words, it should be supposed that the calcination of the catalyst is continued and completed during this period under conditions near to those applied by us (72 h at 480 °C).

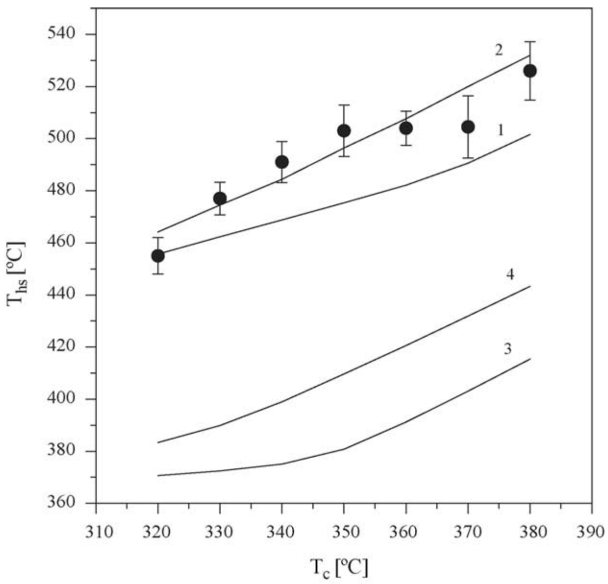

Fig. 3. Influence of the cooling temperature T_c on the hot spot temperature T_{hs}. Filled circles: experimental temperatures in the pilot reactor ($r = 0$) at $V = 4.5$ m^3(STP) h^{-1}, $C_{A,0} = 24$ g m^{-3}(STP), $T_0 = 370$ °C. Curves: model predictions as in the experiments; curve 1: calcined catalyst, energies of activation E_m determined by means of all experimental dependencies (Table 1, column 4), $F_A = 1$ (0–280 cm); curve 2: calcined catalyst, E_m determined by means of the dependence $T_{hs} = f(T_c)$, $F_A = 1$ (0–280 cm); curve 3: pretreated catalyst, $F_A = 0.8$ (0–60 cm), $F_A = 1$ (60–280 cm); curve 4: pretreated catalyst, $F_A = 2$ (0–280 cm).

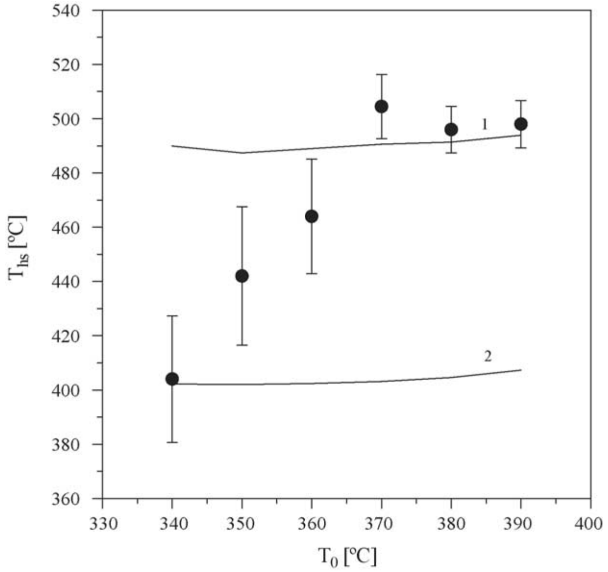

Fig. 4. Dependence of the hot spot temperature T_{hs} on the inlet gas temperature T_0. Filled circles: experimental temperatures in the pilot reactor ($r = 0$) at $V = 4.5$ m^3(STP) h^{-1}, $C_{A,0} = 24$ g m^{-3}(STP), $T_c = 370$ °C. Curves: model predictions under conditions as in the experiments; curve 1: calcined sample, E_m as in column 4 of Table 1, $F_A = 1$ (0–280 cm); curve 2: pretreated catalyst, $F_A = 0.8$ (0–60 cm), $F_A = 1$ (60–280 cm).

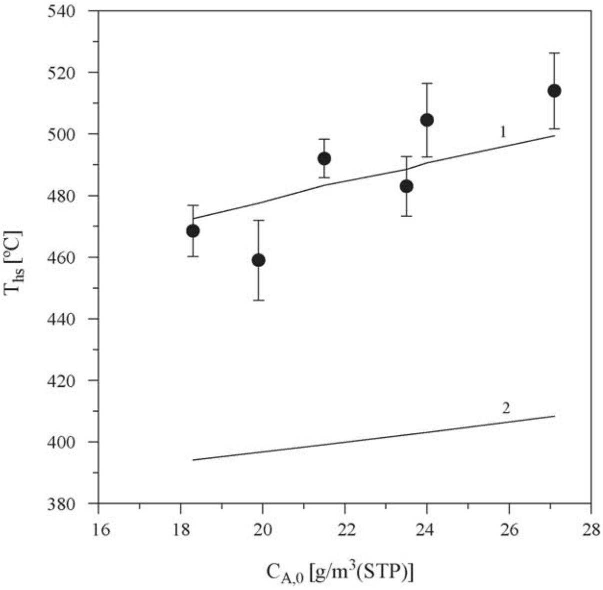

Fig. 5. Experimental and predicted hot spot temperatures T_{hs} as a function of the inlet reagent concentration $C_{A,0}$. Filled circles: experimental temperatures in the pilot reactor ($r = 0$) at $V = 4.5\,m^3(STP)\,h^{-1}$, $T_0 = 370\,°C$, $T_c = 370\,°C$. Curves: model predictions under conditions as in the experiments; curves 1 and 2: as in Fig. 4.

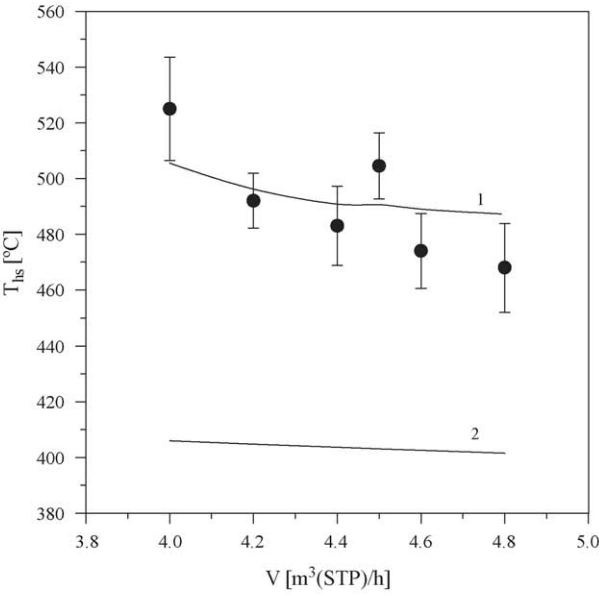

Fig. 6. Effect of the gas flow rate V on the hot spot temperature T_{hs}. Filled circles: experimental temperatures in the pilot reactor ($r = 0$) at $C_{A,0} = 24\,g\,m^{-3}(STP)$, $T_0 = 370\,°C$, $T_c = 370\,°C$. Curves: model predictions under conditions as in the experiments; curve 1: $T_c = 370\,°C$. Curves: model predictions under conditions as in the experiments; curves 1 and 2: as in Fig. 4.

Table 2
Characterization of a non-pretreated catalyst O 4-25 calcined under various conditions

Treatment conditions		Amount of chemically bonded V_2O_5 (wt%)	Amount of chemically unbounded V_2O_5 (wt%)
Time (h)	Temperature (°C)		
4	380	5.40	94.60
72	440	6.31	93.69
24	480	8.32	91.68
72	480	8.67	91.33

But according to the simulation results, the catalyst activity grows up to 1.1 relative units only, while even at an activity two times higher (Fig. 3, curve 4) the predicted temperatures are considerably lower than the experimental ones. Therefore, it seems that the sample treated during 72 h at 480 °C has kinetic parameters, which differ from the original ones [15]. There is a reason to suppose this, because the calcination is carried out by air free of *o*-xylene. Most likely this method of calcination stimulates significantly the amount of vanadium chemically bonded with the TiO_2 support. On the contrary, in the case of an additional calcination taking place in the industrial reactor during the first three days of the real pretreatment (Fig. 2, curve 1), the presence of *o*-xylene suppresses the delicate process [16] of formation of the V_2O_5 monolayer. Obviously, the agent used in the calcination, as well as the temperature and the duration of this process [33] are determinative for the catalyst properties. An additional confirmation of our assumption is a part of the experimental results shown in [16]. According to it, the calcination of a catalyst treated preliminary with *o*-xylene cannot ensure a normal activity of the sample.

The assumption that the amount of the chemically bonded vanadium depends directly proportional on the increase of both the time and the calcination temperature is demonstrated by the experimental results presented in Table 2. It is seen that if both factors increase (Table 2, columns 1 and 2) the content of this vanadium form increases, too. So, a sample treated under the conditions specified (Table 2, column 3, line 4) shows a quantity of the chemically bonded vanadium, which is with about 60% higher than that in a catalyst calcined in the industrial apparatus (Table 2, column 3, line 1). This is an undoubted evidence of the significantly higher activity of the form discussed.

Considering the facts and arguments stated above, we tried to specify kinetic parameters giving a satisfactory approximation to the experimental hot spot temperatures. The kinetic scheme and model of Calderbank et al. [15] were not changed. Besides, we decided to search for new energies of activation, since it was established (Fig. 3, curve 4) that a significant change of the pre-exponential factors had a small effect on the predicted temperatures. Solving an identification problem we determined the new E_m. An optimization procedure based on the method of “fortuity search” and explained in details in [35] was used. According to it random numbers serve as directional derivatives of a vector in whose direction the minimum of the optimisation function is required. The sum of the squares of the differences between experimental and predicted hot spot temperatures is minimised. All experimental results regarding the influence of T_c, T_0, $C_{A,0}$ and V

on the hot spot temperature (25 experiments) are used in the search process. The energies of activation determined in this way are shown in column 4 of Table 1. The pre-exponential factors $K_{0,m}$ do not change and remain equal to the original ones shown in column 2 of Table 1.

So, curve 1 in Fig. 3 represents the temperatures predicted by the heterogeneous model using the new E_m. It is worth noting that in Figs. 2–6 the predicted temperatures are arithmetic means of the temperatures of the gas and solid phases and are related to the centre of the fixed bed ($r = 0$). As seen, the calculated curve lies systematically under the experimental results, while the maximum difference between measured and predicted temperatures (at $T_c = 350\,^{\circ}\mathrm{C}$) reaches 27 °C, or it is below 6%. How far such a description is adequate to the physical experiments is discussed below. Unfortunately, using all experiments we do not succeed in specifying a set of E_m giving a better agreement between curve 1 and the experimental points. Largely this is due to the experimental accuracy, but the kinetic scheme and the model of Calderbank et al. [15] have also a certain influence. As mentioned, they are not deprived of shortcomings. It can be seen in Fig. 3 that curve 2 gives a considerably better approximation to the experimental results. It is obtained with a set of energies of activation, which is also a result of solution of the identification problem, but using only the experimental dependence of the hot spot temperature on the cooling temperature (seven experiments). In this case the values of E_m are lower than E_m in the set specified by all experiments (Table 1, column 4). But they fall into the confidential limits of the final set of energies of activation, and we do not show them here.

Fig. 4 shows the hot spot temperatures T_{hs} as a function of the inlet gas temperature T_0. Curve 1 gives the model prediction with the new energies of activation, while curve 2 represents the same temperatures but for a catalyst pretreated under industrial conditions. It can be seen that, as the inlet temperature increases, the hot spot corresponds first to a catalyst behaving as if it was pretreated (i.e. partly reduced), and gradually to temperatures corresponding to a catalyst being calcined. This could be due to the reoxidation of the V^{3+} and/or V^{4+} to V^{5+}. As V^{5+} are more active than V^{4+} toward *o*-xylene oxidation this would be quite normal. But another explanation is also possible. It seems that curve 1 describes comparatively well the experiments, but if the points at $T_0 = 340$ and 350 °C are eliminated. As they (especially the first one) are closer to the model prediction for a pretreated sample (curve 2), these points could be considered as not typical of the form calcined under the conditions applied (480 °C, 72 h).

It is interesting here to discuss the minimum of the hot spot temperature ($T_{\mathrm{hs}} = 487.4\,^{\circ}\mathrm{C}$) for the calcined catalyst (curve 1). It is located at $T_0 = 350\,^{\circ}\mathrm{C}$. This result agrees qualitatively (to a great extent also quantitatively) with our experimental study [22]. According to it, the hot pot temperature of a pretreated catalyst has a minimum value at initial gas temperatures lower by about 10–15 °C than that of the coolant.

Figs. 5 and 6 display the experimental and predicted hot spot temperatures of both catalyst forms (calcined and pretreated) as a function of the inlet reagent concentration $C_{\mathrm{A},0}$ (Fig. 5) and the gas flow rate V (Fig. 6). Curve 1 in both figures is related to the model solutions obtained by the new E_m, while curve 2 demonstrates the behaviour of a pretreated sample. For both dependencies it can be maintained that the new kinetic parameters reproduce well the experimental temperatures of the hot spot. In this two cases also, the catalyst calcined in the way discussed shows considerably higher temperature regimes in comparison with those of the completely pretreated form. Under certain conditions they exceed the maximum admissible temperature for the catalyst (500 °C). A comparison of curves 1 and 3 in Fig. 3 and 1 and 2 in Figs. 4–6 shows almost the same course of the curves for both catalyst forms. This indicates that the coefficients of parametric sensitivity of these forms are practically identical in the interval of changing the process parameters. As the values mentioned are low, there is no risk to realise the process by using a pretreated catalyst, which is discussed in detail in [10]. But due to the high temperatures obtained by a calcined sample, it cannot be used in the industry. Regardless of the low coefficient of PS, small accidental variations of the parameters could lead to temperatures exceeding the maximum admissible one for the system V_2O_5–TiO_2, and hence to its thermal deactivation (sintering) in the hot spot region. An uncontrolled running of the process accompanied by a heat explosion is also possible.

The specified energies of activation valid for the calcined catalyst enable the engineer to prognosticate the temperature regime produced by this form under various industrial conditions and a special organisation of the bed. For instance, if the conventional technological conditions ($T_c = 370\,^{\circ}\mathrm{C}$, $T_0 = 230\,^{\circ}\mathrm{C}$, $V = 4.5\,\mathrm{m}^3(\mathrm{STP})\,\mathrm{h}^{-1}$ and $C_{\mathrm{A},0} = 40\,\mathrm{g\,m}^{-3}(\mathrm{STP})$) are used, the hot spot temperature of the non-pretreated sample increases to 552 °C. Obviously, such a technological regime cannot be applied in the industry. But if the fixed bed is properly organised, namely if both forms are combined together, a calcined catalyst could find industrial application. These opportunities will be shown in a next paper.

It is worth discussing the ratios of the original energies of activation (Table 1, column 3; catalyst calcined industrially at 380 °C during 4–6 h) to the new ones (Table 1, column 4; catalyst calcined 72 h at 480 °C). They varies between 1.488 ($E_{1,\mathrm{original}}/E_{1,\mathrm{new}}$) and 1.765 ($E_{2,\mathrm{original}}/E_{2,\mathrm{new}}$), while the arithmetic mean of all ratios is 1.604. At the same time the amount of the chemically bonded V_2O_5 in a catalyst calcined at 480 °C during 72 h (Table 2, column 3; 8.67 wt.%) is 1.606 times higher than that one in a sample calcined industrially (Table 2, column 3; 5.40 wt.%). In other words the mean reduction of E_m for the form calcined during 72 h at 480 °C corresponds exactly to the increased content of the chemically bonded V_2O_5 in the same form.

Table 3
Estimation of experimental and predicted results

Number	Dependence $T_{hs} = f(T_c)$ (Fig. 3, curve 1)	Dependence $T_{hs} = f(T_0)$ (Fig. 4, curve 1)		Dependence $T_{hs} = f(C_{A,0})$ (Fig. 5, curve 1)	Dependence $T_{hs} = f(V)$ (Fig. 6, curve 1)
		With all points	Without two points		
F	3.51	13.20	1.22	1.12	1.60
F_t	19.44	19.44	19.43	19.44	19.44

5.4. *Statistic analysis of the experimental and predicted results*

Each of the experimental results shown in Figs. 3–6 is performed three times. The confidential intervals of the different experiments are determined on this basis. As seen in the figures, the reproducibility of each point is different. The best repeatability of the experiments (lowest variance of reproducibility $(\sigma_{n-1})^2$) is registered for the mean values of the hot spot $T_{hs} = 477\,^\circ C$ at $T_c = 330\,^\circ C$ (Fig. 3) and $T_{hs} = 492\,^\circ C$ at $C_{A,0} = 21.5\,g\,m^{-3}$(STP) (Fig. 5). The worst repeatability (highest variance of reproducibility $(\sigma_{n-1})^2$) is observed for $T_{hs} = 442\,^\circ C$ at $T_0 = 350\,^\circ C$ (Fig. 4). With a view to estimate more precisely the adequacy of the predicted results, the Fiescher number is calculated by using the best reproducibility of the experimental results ($(\sigma_{n-1})^2 = \min$).

As seen in Figs. 3–6, highest differences between experiments and predictions (highest variance $(S_r)^2$) exist for the dependence of the hot spot temperature on inlet gas temperature (Fig. 4). Certainly, this statement is valid if all experimental points in Fig. 4 (six experiments) are considered. But, as discussed, the hot spot temperatures at $T_0 = 340$ and $350\,^\circ C$ are rather unreliable and could be neglected. On the other hand both the heterogeneous model and the kinetic model with the specified energies of activation give the best approximation to the experimental hot spots ($(S_r)^2 = \min$) in the case $T_{hs} = f(C_{A,0})$ (Fig. 5). The dependencies $T_{hs} = f(T_c)$ (Fig. 3) and $T_{hs} = f(V)$ (Fig. 6) have an intermediate position, but obviously the variance of the first one is higher than the variance of the second.

The calculated values of the Fiescher number (F), as well as its tabulated values (F_t) at ranges of discretion $\nu_1 = 20$ (or $\nu_1 = 18$ after eliminating two points in Fig. 4) and $\nu_2 = 2$ (three times reiteration of all experiments) are presented in Table 3. As known, the values 20 and 18 for ν_1 are the differences between the number of the experiments (25 and 23, respectively) and the number of the energies of activation (E_1–E_5) specified by using these experiments.

It can be seen in Table 3 that all experimental dependencies (Figs. 3–6) are adequately interpreted by both the heterogeneous model and the kinetic model of Calderbank et al. [15] with the new energies of activation. This is confirmed by the calculated values of the Fiescher number F (Table 3, first line). For dependencies $T_{hs} = f(T_c)$ (Fig. 3), $T_{hs} = f(C_{A,0})$ (Fig. 5) and $T_{hs} = f(V)$ (Fig. 6) they are considerably lower than the corresponding tabulated values F_t (Table 3, second line). For the dependence $T_{hs} = f(T_0)$ (Fig. 4; all experimental points included) only, the calculated (13.20) and the tabulated (19.44) values are closer to each other. But after eliminating the disputable two points, the calculated Fiescher number drops sharply to 1.22.

6. Conclusions

The study of the behaviour of the V_2O_5–TiO_2 (anatase) supported catalyst O 4-25 calcined under special conditions allows the following conclusions and results to be defined.

1. Energies of activation valid for a calcined catalyst are specified.
2. The heterogeneous two-dimensional mathematical model and the kinetics by Calderbank et al. [15] with the new energies of activation describe adequately the experimental hot spot temperatures in a fixed bed composed by a calcined catalyst.
3. The characteristics of the catalyst depend essentially on both the duration and the temperature of thermal treatment (calcination), as well as on the presence of *o*-xylene in the oxidation agent.
4. The specified conditions of thermal treatment of the catalyst lead to a significant increase of the chemically bonded vanadium in comparison with the traditional calcination in the industry.
5. The average reduction of the new energies of activation (in comparison with the original ones) corresponds exactly to the increased amount of the chemically bonded vanadium in a catalyst calcined under special conditions.
6. The original kinetic scheme and the kinetic parameters of Calderbank et al. [15] predicts in a satisfactory way the behaviour of a catalyst calcined and pretreated under industrial conditions.
7. Regardless of the low parametric sensitivity of the catalyst calcined 72 h at 480 °C, it cannot be used in the industry due to its high activity. But there are interesting opportunities to use effectively this form, if it is combined with a pretreated catalyst, namely if a dual catalyst bed is organized. In the case of loading the high active form (only calcined catalyst) in the second half of the bed, where the temperature is comparatively low, the reoxidation of the side products into phthalic anhydride should be significantly intensified.

References

[1] C.R. Dias, M.F. Portela, G.C. Bond, Synthesis of phthalic anhydride: catalysis, kinetics and reaction modeling, Catal. Rev. Sci. Eng. 39 (1997) 169.

[2] J.N. Papageorgiou, G.F. Froment, Phthalic anhydride synthesis. Reactor optimization aspects, Chem. Eng. Sci. 51 (1996) 2091.

[3] W. Krajewski, M. Galantowicz, Effect of catalyst deactivation on the process of oxidation of *o*-xylene to phthalic anhydride in an industrial multitubular reactor, Stud. Surf. Sci. Catal. 126 (1999) 447.

[4] M. Galantowicz, Phthalic anhydride-important product of the organic industry, in: Proceedings of the 12th International Congress of Chemical and Process Engineering, CHISA-96, Prague, Czech Republic, 23–30 August 1996, MAPRET lecture, pp. 1–25.

[5] A.I. Anastasov, An investigation of the kinetic parameters of the *o*-xylene oxidation process carried out in a fixed bed of high-productive vanadia–titania catalyst, Chem. Eng. Sci. 58 (2003) 89.

[6] V. Nikolov, D. Klissurski, A. Anastasov, Phthalic anhydride from *o*-xylene catalysis: science and engineering, Catal. Rev. Sci. Eng. 33 (1991) 319.

[7] V.A. Nikolov, A.I. Anastasov, A study of coolant temperature in an industrial reactor for *o*-xylene oxidation, AIChE J. 35 (1989) 511.

[8] A.I. Anastasov, V.A. Nikolov, A catalyst deposited over the external surface of the reactor tubes—a new solution for carrying out heterogeneous catalytic processes, Can. J. Chem. Eng. 80 (2002) 79.

[9] A.I. Anastasov, Deactivation of an industrial V_2O_5–TiO_2 catalyst for oxidation of *o*-xylene into phthalic anhydride, Chem. Eng. Process. 42 (2003) 449.

[10] A.I. Anastasov, A study of the influence of the operating parameters on the temperature of the hot spot in a fixed bed reactor, Chem. Eng. J. 86 (2002) 287.

[11] R.J. van Welsenaere, G.F. Froment, Parametric sensitivity and runaway in fixed bed catalytic reactors, Chem. Eng. Sci. 25 (1970) 1503.

[12] V. Balakotaiah, D. Kodra, D. Nguyen, Runaway limits for homogeneous and catalytic reactors, Chem. Eng. Sci. 50 (1995) 1149.

[13] J.C. Pirkle, I.E. Wachs, Activity profiling in catalytic reactors, Chem. Eng. Progr. 83 (1987) 29.

[14] C.R. Dias, M.F. Portela, G.C. Bond, Oxidation of *o*-xylene to phthalic anhydride over V_2O_5/TiO_2 catalysts. Part 4. Mathematical modelling study and analysis of the reaction network, J. Catal. 164 (1996) 276.

[15] P.H. Calderbank, K. Chandrasekharan, C. Fumagalli, The prediction of the performance of packed-bed catalytic reactors in the air-oxidation of *o*-xylene, Chem. Eng. Sci. 32 (1977) 1435.

[16] V.A. Nikolov, A.I. Anastasov, Pretreatment of a vanadia–titania catalyst for partial oxidation of *o*-xylene under industrial conditions, Ind. Eng. Chem. Res. 31 (1992) 80.

[17] A.I. Anastasov, V.A. Nikolov, Optimal policies of operation of a fixed-bed reactor for oxidation of *o*-xylene into phthalic anhydride, Ind. Eng. Chem. Res. 37 (1998) 3424.

[18] G.F. Froment, Fixed-bed catalytic reactors. Technological and fundamental aspects, Chem. Ing. Technol. 46 (1974) 374.

[19] M.M.J. Quina, R.M. Quinta Ferreira, Thermal runaway conditions of a partially diluted catalytic reactor, Ind. Eng. Chem. Res. 38 (1999) 4615.

[20] L.S. Kershenbaum, F. López-Isunza, Dynamic behavior of an industrial scale fixed-bed reactor, in: Proceedings of the 7th International Symposium on Chemical Reaction Engineering, Boston, USA, 4–6 October 1982, American Chemical Society—Symposium Series, vol. 196, 1982, pp. 109–119.

[21] L. Lapidus, N.R. Amundson (Eds.), Chemical Reactor Theory, Prentice-Hall Inc., Englewood Cliffs, NJ, 1977, a review (Chapter 6).

[22] V.A. Nikolov, A.I. Anastasov, Influence of the inlet temperature of the performance of a fixed-bed reactor for oxidation of *o*-xylene into phthalic anhydride, Chem. Eng. Sci. 47 (1992) 1291.

[23] As. Anastasov, D. Elenkov, V. Nikolov, A model study of a conventional fixed bed tubular reactor with a catalyst layer on the inside tube wall, Chem. Eng. Process. 23 (1988) 203.

[24] F. López-Isunza, E. Martinez, L.S. Kershenbaum, Non-stationary catalyst activity profiles in fixed bed reactors for partial oxidation, in: Proceedings of the 37th Canadian Chemical Engineering Conference, Montreal Canada, 18–22 May 1987.

[25] J. Skrzypek, M. Grzesik, M. Galantowicz, J. Solinski, Kinetics of the catalytic air oxidation of *o*-xylene over a commercial V_2O_5–TiO_2 catalyst, Chem. Eng. Sci. 40 (1985) 611.

[26] R.Y. Saleh, I.E. Wachs, S.S. Chan, C.C. Chersich, The interaction of V_2O_5 with TiO_2 (anatase): catalyst evolution with calcination temperature and *o*-xylene oxidation, J. Catal. 98 (1986) 102.

[27] B. Olthov, A. Khodakov, A. Bell, E. Iglesia, Effect of support composition and pretreatment conditions on the structure of vanadia dispersed on SiO_2, Al_2O_3, TiO_2, ZrO_2 and HfO_2, J. Phys. Chem. B 104 (2000) 1516.

[28] G. Bond, Preparation and properties of vanadia–titania monolayer catalysts, Appl. Catal. A 157 (1997) 91.

[29] B. Grzybowska-Swierkocz, Vanadia–titania catalysts for oxidation of *o*-xylene and other hydrocarbons (Review), Appl. Catal. A 157 (1997) 263.

[30] G. Bond, What limits the selectivity attainable in the catalysed oxidation of *o*-xylene to phthalic anhydride? J. Chem. Technol. Biotechnol. 68 (1997) 6.

[31] C.R. Dias, M.F. Portela, G.C. Bond, Oxidation of *o*-xylene to phthalic anhydride over V_2O_5/TiO_2 catalysts. I. Influence of catalyst composition, preparation method and operating conditions on conversion and product selectivities, J. Catal. 157 (1995) 344.

[32] I.E. Wachs, S.S. Chan, R.Y. Saleh, The interaction of V_2O_5 with TiO_2 (anatase). II. Comparison of fresh and used catalysts for *o*-xylene oxidation to phthalic anhydride, J. Catal. 91 (1985) 366.

[33] M. del Arco, M. Jesús Holgado, C. Martin, V. Rives, Effect of thermal treatments on the properties of V_2O_5/TiO_2 and MoO_3/TiO_2 systems, J. Catal. 99 (1986) 19.

[34] P. Sadhukhan, E.E. Petersen, Oxidation of naphthalene in packed-bed reactor with catalyst activity profile: a design scheme for improved reactor stability and higher product yield, AIChE J. 22 (1976) 808.

[35] A.S. Shmelyov, A.I. Anastasov, An investigation of the kinetics of anthracene oxidation over a complex vanadium catalyst, Comm. Dept. Chem. -BAS 9 (1976) 361 (in Bulgarian).